

Research Articles | Behavioral/Cognitive

Characterizing directional dynamics of semantic prediction based on inter-regional temporal generalization

<https://doi.org/10.1523/JNEUROSCI.0230-24.2025>

Received: 1 February 2024
Revised: 7 February 2025
Accepted: 11 February 2025

Copyright © 2025 the authors

This Early Release article has been peer reviewed and accepted, but has not been through the composition and copyediting processes. The final version may differ slightly in style or formatting and will contain links to any extended data.

Alerts: Sign up at www.jneurosci.org/alerts to receive customized email alerts when the fully formatted version of this article is published.

1 **Characterizing directional dynamics of semantic prediction based on**
2 **inter-regional temporal generalization**

3

4 **Abbreviated title:** Directional dynamics of semantic prediction

5

6 Fahimeh Mamashli¹, Sheraz Khan¹, Elaheh Hatamimajoumerd², Mainak Jas¹, Işıl Uluç¹, Kaisu
7 Lankinen¹, Jonas Obleser³, Angela D. Friederici⁴, Burkhard Maess⁵, Jyrki Ahveninen¹

8

9 ¹Department of Radiology, Massachusetts General Hospital, Athinoula A. Martinos Center for
10 Biomedical Imaging, Harvard Medical School, Boston, MA 02129.

11 ²Department of Electrical and Computer Engineering, Northeastern University, Boston, MA
12 02115.

13 ³Department of Psychology, University of Lübeck, Lübeck 23562, Germany.

14 ⁴Department of Neuropsychology, Max Planck Institute for Human Cognitive and Brain Sciences,
15 Leipzig 04103, Germany.

16 ⁵MEG and Cortical Networks Group, Max Planck Institute for Human Cognitive and Brain
17 Sciences, Leipzig 04103, Germany.

18

19 **Corresponding authors:** Fahimeh Mamashli, *Email:* fmamashli@mgh.harvard.edu, Jyrki
20 Ahveninen, *Email:* jahveninen@mgh.harvard.edu, Phone: +1 617 643 5634, Address: 149 13th
21 Street, Charlestown, MA 02129

22

25

26 **Number of pages:** 25

27 **Number of figures:** 6

28 **Number of words for abstract:** 250

29 **Number of words for introduction:** 692

30 **Number of words for discussion:** 1119

31

32 **Acknowledgements:** This research was supported by the Max Planck Society, the International
33 Max Planck Research School Leipzig and by NIH grants: R01DC016915, R01DC016765,
34 R01DC017991, P41EB015896. We thank Yvonne Wolff for help in acquiring the data.

35

36 **Declaration of Competing Interests:** The authors declare no competing financial interests.

37

38

39

40 **Abstract**

41 The event-related potential/field component N400(m) is a widely accepted neural index for
42 semantic prediction. Top-down input from inferior frontal areas to perceptual brain regions is
43 hypothesized to play a key role in generating the N400, but testing this has been challenging due
44 to limitations of causal connectivity estimation. We here provide new evidence for a predictive
45 model of speech comprehension in which IFG activity feeds back to shape subsequent activity in
46 STG/MTG. Magnetoencephalography (MEG) data was obtained from 21 participants (10 men, 11
47 women) during a classic N400 paradigm where the semantic predictability of a fixed target noun
48 was manipulated in simple German sentences through the preceding verb. To estimate causality,
49 we implemented a novel approach, based on machine learning and temporal generalization, to
50 test the effect of inferior frontal gyrus (IFG) on temporal regions. A support vector machine (SVM)
51 classifier was trained on IFG activity to classify less predicted (LP) and highly predicted (HP)
52 nouns and tested on superior/middle temporal gyri (STG/MTG) activity, time-point by time-point.
53 The reverse procedure was then performed to establish spatiotemporal evidence for or against
54 causality. Significant decoding results were found in our bottom-up model, which were trained at
55 hierarchically lower level areas (STG/MTG) and tested at the hierarchically higher IFG areas.
56 Most interestingly, decoding accuracy also significantly exceeded chance level when the classifier
57 was trained on IFG activity and tested on successive activity in STG/MTG. Our findings indicate
58 dynamic top-down and bottom-up flow of information between IFG and temporal areas when
59 generating semantic predictions.

60

61 **Significance Statement**

62 Semantic prediction helps anticipate the meaning of upcoming speech based on
63 contextual information. How frontal and temporal cortices interact to enable this crucial function
64 has remained elusive. We used novel data-driven MEG analyses to infer information flow from
65 lower to higher areas (bottom-up) and vice versa (top-down) during semantic prediction. Using
66 "earlier" MEG signals in one area to decode the "later" in another, we found that inferior frontal
67 cortices feed predictions back to temporal cortices, to help decipher bottom-up signals going to
68 the opposite direction. Our results provide experimental evidence on how top-down and bottom-
69 up influences interact during language processing.

70

JNeurosci Accepted Manuscript

71 Introduction

72 Lexical semantic prediction has been associated with an event-related response
73 component termed N400 (Kutas and Hillyard, 1980, 1989; Federmeier, 2007; Lau et al., 2009;
74 Lau et al., 2013b; Lau et al., 2013a). N400 amplitude is sensitive to the previous context, and its
75 amplitude is reliably reduced following a supportive or predictive context (Kutas and Hillyard,
76 1984; Federmeier et al., 2007; Kutas and Federmeier, 2011; Wlotko and Federmeier, 2012).

77 Using MEG, several approaches have been taken to identify the brain network underlying
78 the N400m, the magnetic counterpart of N400 observed in EEG. Generally, the results suggest
79 left hemispheric dominance and involvement of temporal and inferior frontal sources in N400(m)
80 generation (Halgren et al., 2002; Marinkovic et al., 2003; Pulvermüller et al., 2005; Maess et al.,
81 2006; Pylkkanen and McElree, 2007; Salmelin, 2007; Dikker and Pylkkanen, 2012). Despite
82 numerous studies on N400, the information flow between regions appearing to contribute to N400
83 generation has remained elusive.

84 Theoretical models on language processing suggest that superior and middle temporal
85 regions perform bottom-up processing while inferior frontal areas send top-down (or feedback) to
86 temporal areas to support lexical-semantic processing (Engel et al., 2001; Badre et al., 2005;
87 Badre and Wagner, 2007; Lau et al., 2008). This proposition receives support from studies using
88 dynamic causal modeling (DCM) of fMRI activations during semantic processing (Noppeney et
89 al., 2006) though the exact timing of these processes needs further specification. In
90 neurophysiological studies, these kinds of directional or "causal" influences are often
91 characterized as effective connectivity. However, due to methodological challenges of causality
92 estimation from MEG or EEG data, testing hypotheses regarding the interregional influences
93 during N400 generation has remained difficult.

94 A small number of previous N400 studies have estimated fronto-temporal directional
95 influences using a model-driven method known as Granger causality (Cope et al., 2017;
96 Schoffelen et al., 2017). The Granger causality analysis tests whether information from the past

97 activity of one region can predict future activity in another better than its own past using single
98 variable auto-regressive models (Granger and Hatanaka, 1964). For example, in an MEG
99 experiment with word reading task, the Granger causality method identified that inferior frontal
100 cortex and anterior temporal regions to receive widespread input from language network and
101 middle temporal regions to send widespread output to fronto-temporal-parietal cortex (Schoffelen
102 et al., 2017) . In parallel, bi-directional Granger-causal relationships were observed between
103 temporal and frontal sources in matching between degraded spoken words with the previously
104 shown visual word (Cope et al., 2017). However, the limitation of model-driven approaches such
105 as Granger causality, or its analogue "dynamic causal modeling", is that they require assumptions
106 of the temporal and spatial covariance of the sources, which are difficult to estimate in the
107 presence of noise and with a limited amount of data.

108 Here, to address the critical barriers on causality modeling, we therefore implemented a
109 novel data-driven approach to estimate the causal connections between frontal and temporal
110 areas during N400 generation. We used data from a classic N400 paradigm with simple German
111 sentences where the final noun was highly predicted (HP) or less predicted (LP) by the preceding
112 verb. Nouns are identical in both conditions, but the prior context varies. Hence, HP and LP are
113 characteristics of nouns-in-context and not a (lexical) characteristics of the nouns themselves.
114 The same noun can be highly predictable in one context and have a low predictability in another
115 context. Our method is based on the temporal generalization technique (King and Dehaene,
116 2014), which uses machine learning. Using this method a classifier is trained on one cortical
117 area's activity and each time point to discriminate between HP and LP. This classifier is then
118 tested in another cortical area across all time points following temporal generalization idea.

119 This method allows us to quantify that how much information from one area is predictive
120 of activity in another area and future time points. Our method's concept is, thus, similar to Granger
121 causality in principle but it is predominantly data driven and based on multivariate analysis. We
122 tested this method in the context of a study pursuing better understanding of the complex

123 dynamics of top-down and bottom-up information flow within fronto-temporal language network
124 during auditory perception of speech.

JNeurosci Accepted Manuscript

125 **Materials and Methods**

126 ***Participants***

127 In total, N=21 right-handed German native speakers (11 women) participated in a MEG
128 experiment (age range: 20-32 years, median: 27) (Oldfield, 1971). The participants reported
129 having no hearing deficits or neurological diseases and they gave a written informed consent
130 before the experiment. The study was conducted in accordance with the declaration of Helsinki,
131 and it received ethical approval from the ethics commission of the University of Leipzig (Ref. 059-
132 11-07032011). Other, more rudimentary results on these data have been analyzed and published
133 previously in (Maess et al., 2016; Mamashli et al., 2019b).

134

135 ***Stimuli***

136 The stimuli consisted of short German sentences, including a pronoun, verb, article and
137 noun [e.g. *He drives the car, German: Er fährt das Auto*], which were grouped based on the cloze
138 probability values of the nouns. Cloze probability is the probability that mother tongue speakers
139 would select this word to complete the given context (Taylor, 1953). Cloze probability was
140 measured in a behavioral pre-study. Participants filled out uncompleted sentences that had a
141 personal pronoun (Er/Sie [he/she]) followed by a verb. Participants were asked to complete the
142 sentence in a simple way by providing just a determiner and a noun. The cloze probability of the
143 nouns was measured by the number of times a native speaker completed the sentence with that
144 noun relative to all other completion for a given verb (Maess et al, 2016). Nouns with a cloze
145 probability >50% were considered as having high semantic predictability (HP), [e.g. *He drives the*
146 *car, German: Er fährt das Auto*] and those with a cloze probability <=24% were considered to
147 have low semantic predictability (LP), [e.g. *He gets the car, German: Er kriegt das Auto*] (Maess
148 et al., 2016). The cut-off thresholds were chosen based on Gunter et al, 2000 study. The complete
149 set of stimuli consists of 69 pairs. Each pair had same noun but different verb to provide the prior

150 context. The verb was either predictive or not predictive of the following noun. As we used the
151 same determiner-noun phrase for each of the sentence pairs, there were no stimulus driven
152 differences such as word frequency or length at the noun level between the conditions.

153 ***Design and procedure***

154 In a dimly lit shielded room, MEG data were measured with a 306 channel Neuromag
155 Vectorview device (Elekta, Helsinki, Finland), at 500 Hz sampling rate using a bandwidth of
156 160 Hz (Vacuumschmelze Hanau, Germany). Each participant's individual hearing thresholds
157 were determined for both ears separately using a subpart of one of the sentences. This particular
158 sentence was not used later in the actual experiment. Stimuli were presented at 48 dB sensation
159 level (i.e., above the mean between left and right ear individual hearing threshold). Each
160 experimental session consisted of five recording blocks. All stimuli were randomized and
161 presented in the first two blocks. Using a different randomization, stimuli were repeated in blocks
162 three and four. The onsets of all sentences, and the onsets of the verbs and the nouns were
163 specifically marked. In the fifth block, a sequence of simple tones (200 ms length and 500 Hz
164 pitch) was presented. The data from this block are not presented here.

165 During each measurement block, participants were instructed to fixate a visually projected
166 cross, to listen carefully to the presented sentences, and to stay motionless. The fixation cross
167 was presented for 700 ms before onset until 700 ms after the offset of each sentence. To keep
168 participants engaged with the listening, in 15% of the sentences, the same or an alternative
169 sentence, was spoken by a male voice. Participants' (incidental) were asked to judge whether the
170 two preceding sentences (female and male voice) were the same by a button press. A symbolic
171 face was provided to inform participant's response-to-button-alignment: one happy and one sad
172 face, presented on the left and right side of the screen. Participants answered "yes" with pressing
173 the button at the side of the happy face and "no" with the other using their thumb. The symbolic
174 faces were randomly presented on right or left and counterbalanced over all stimuli in each block.

175 **Data preprocessing**

176 Signal space separation (SSS) method was used to suppress environmental interference
177 of the MEG data (Elekta-Neuromag Maxfilter software) (Taulu et al., 2004; Taulu and Simola,
178 2006) and also to transform the data from each block into the same head position (Taulu et al.,
179 2004). To suppress cardiac and eye artifacts, signal space projection was used (Gramfort et al.,
180 2014). Data were extracted into single trials lasting 1.4 seconds, ranging from 400 ms before noun
181 onset to 1000 ms following it. MEG data were filtered with a low pass filter of 25 Hz using MNE-
182 C (fft-based filter) and a highpass of 0.5 Hz with a filter size of 8192. Epochs were rejected if the
183 peak-to-peak amplitude exceeded 150 μ V, 1 pT/cm, and 3 pT in any of the electrooculogram,
184 gradiometer, and magnetometer channels, respectively. To equalize the signal-to-noise ratio in
185 each condition (i.e., HP and LP), the number of trials in the lesser populated condition was used
186 to analyze both conditions. The median of the used trials was 97.5 and the minimum number of
187 trials was 79.

188 **Source estimation**

189 Each participant's cortical surface representation was reconstructed from 3D structural
190 MRI data using FreeSurfer (<http://surfer.nmr.mgh.harvard.edu>). The cortical surface was
191 decimated to a grid of 10242 dipoles per hemisphere, i.e., with approximate spacing of 5 mm
192 between adjacent source locations on the cortical surface. The MEG forward solution was
193 computed using a single-compartment boundary-element model (BEM) assuming the shape of
194 the intracranial space (Hämäläinen and Sarvas, 1987). The inner skull surface triangulations was
195 generated from the T1-weighted MR images of each participant with the Freesurfer "watershed"
196 algorithm. The cortical current distribution was estimated using a depth-weighted, minimum-norm
197 estimate (MNE) (<http://www.martinos.org/martinos/userInfo/data/sofMNE.php> (Lin et al., 2006))
198 assuming a fixed orientation of the source, perpendicular to the individual cortical mesh. The
199 noise-covariance matrix used to calculate the inverse operator was estimated from data collected
200 from empty room recordings prior and following the recordings with each subject. To reduce the

201 bias of the MNEs towards superficial currents, we used depth weighting. In other words, the
202 source covariance matrix was adjusted to favor deep source locations.

203 ***Inter-subject cortical surface registration for group analysis***

204 Each participant's inflated cortical surface was registered to an average cortical
205 representation (FsAverage in FreeSurfer) by optimally aligning individual sulcal-gyral patterns
206 computed in FreeSurfer (Fischl et al., 1999a). To provide more accurate inter-subject alignment
207 of cortical regions than volume-based approaches, we used a surface-based registration
208 technique based on folding patterns (Fischl et al., 1999b; Van Essen and Dierker, 2007).

209 ***Region identification and analysis***

210 The analysis were focused on six cortical areas of the FreeSurfer Desikan-Killiany Atlas
211 in both hemispheres, which are believed to constitute the most critical parts of semantic language
212 networks (Lau et al., 2008; Price, 2010; Friederici, 2011), including bilateral superior temporal
213 gyrus (STG), middle temporal gyrus (MTG), and inferior frontal gyrus (IFG) including Brodmann
214 areas BA44, BA45 and BA47. In addition, we used an automatic routine (mris_divide_parcellation)
215 available in the Freesurfer package (equal size principle) to break each large region into smaller
216 equal size sub-regions; i.e., all sub-regions in all regions were of approximately the same size—
217 thereby increasing the spatial specificity for further analysis (Mamashli et al., 2017; Mamashli et
218 al., 2019a; Mamashli et al., 2019c; Mamashli et al., 2020; Mamashli et al., 2021a; Mamashli et
219 al., 2021b), as areas can lead to temporal signal cancellations. Furthermore, we grouped the sub-
220 regions into anterior and posterior parts of each cortical region, e.g., STG will be divided into
221 anterior STG (aSTG) and posterior STG (pSTG). In total, we had six regions of interest (ROI) in
222 each hemisphere: aSTG, pSTG, aMTG, pMTG, aIFG and pIFG (**Figure 1**).

223

224 ***Sub-region time series extraction***

225 Epochs were extracted and averaged across all vertices within each sub-region, to
226 compute the mean sub-region time course, generating $X(\Lambda, T, N)$, where Λ is the number of
227 vertices, T is the number of time points, and N is the number of epochs. Since the individual vertex
228 (dipole) orientations is ambiguous, these time series were first aligned with the dominant
229 component of the multivariate source time course, and then averaged to calculate the sub-region
230 mean. In order to align the sign of the time series across vertices, we first concatenated all the
231 epochs for each vertex in a single time series and then computed an SVD of the data $\mathbf{X}^T = \mathbf{U}\mathbf{\Sigma}\mathbf{V}^T$.
232 The sign of the dot product between the first left singular vector \mathbf{U} and all other time-series in a
233 sub-region was computed. If this sign was negative, we inverted the time-series before averaging
234 over all time courses of a sub-region. Finally, temporal data of each sub-region was arranged as
235 a 2D matrix [epochs X time].

236 ***Inter-regional temporal generalization Multivariate Pattern Analysis (MVPA)***

237 Here, we use a data-driven multivariate approach to estimate the causal connection
238 between two regions. Multivariate pattern analysis has been used before both using MEG (King
239 and Dehaene, 2014; Cichy and Pantazis, 2017; Mohsenzadeh et al., 2018; Hatamimajoumerd et
240 al., 2020) and fMRI (Hatamimajoumerd et al., 2022) , where a classifier is trained in one
241 experimental condition and tested in another condition. In contrast, here, a classifier is trained to
242 learn the difference between conditions at one point of time in one region and then tested in at
243 another point of time in another region.

244 To accomplish this, an SVM classifier is trained across two conditions (LP vs HP) in ROI₁
245 using the sub-ROI activities as features at each time point. This classifier is then tested in ROI₂
246 and across all time points using temporal generalization idea. This process is replicated for all
247 time points of ROI₁, and eventually provides the temporal generalization matrix for each ROI pair.
248 To increase the signal-to-noise ratio, we randomly selected 10 epochs, averaged within each
249 condition, and bootstrapped this 100 times (Cichy and Pantazis, 2017). Different randomizations

250 were done in ROI₁ and ROI₂. The time window was from -200ms to 800ms. We focused our
251 analysis on the within hemisphere ventral and dorsal path in language processing to investigate
252 the information flow from anterior IFG to anterior temporal areas (e.g., aIFG to aSTG/aMTG) and
253 posterior IFG to posterior temporal (e.g., pIFG to pSTG/pMTG). Similarly, we tested the opposite
254 direction from temporal to IFG (e.g., pSTG/pMTG to pIFG). For simplicity, we refer these patterns
255 to as "directional connections". In total, we tested eight directional connections in each
256 hemisphere. A schematic display of the method is shown in **Figure 2**.

257

258 ***Dissociating directional information from sustained activity***

259 To further investigate our interpretation of top-down and bottom-up dynamics, we
260 conducted an additional analysis to test the null hypothesis that for each connection top-down
261 and bottom-up effects are equal in all times and do not provide any directional information. The
262 Pearson correlation of the decoding accuracies of top-down (trained in frontal and tested in
263 temporal) and bottom-up effect (trained in temporal and tested in frontal) across all subjects for
264 each connection was calculated. If the null hypothesis were true, we would expect a strong
265 correlation between the two, as both top-down and bottom-up occur in the same time interval;
266 that is, sustained activity, i.e. decoding accuracy has a squared shape and does not provide any
267 directional information. Conversely, if the null hypothesis were rejected, top-down and bottom-up
268 could exhibit distinct temporal patterns, which would indicated that there is valid directional
269 information.

270

271 ***Statistical analysis***

272 ***(A) Inter-regional temporal generalization MVPA***

273 For each directional connectivity between a pair of ROIs, cluster-based statistics were
274 applied (Maris and Oostenveld, 2007). We used $P < 0.025$ as the initial threshold, 1000

275 permutations, and one-tailed one-sample t-tests as the test statistics against the chance level for
276 binary classifier. We estimated the empirical chance level using simulations by shuffling the labels
277 100 times and performed the temporal generalization for all subjects and connections. The
278 temporal generalization matrix was flattened and gained 10000 shuffled accuracies. To generate
279 a null distribution, values were pooled across all subjects and connections. The null distribution
280 was Gaussian with mean at 0.5. Therefore, the empirical chance level for our case was 0.5. Thus,
281 we used 0.5 as the chance level in our test statistic. In addition, to correct for 16 directional
282 connectivity tests, we applied false discovery rate (FDR) method at 0.025 thresholds. The 0.025
283 thresholds were chosen to account for the one-tailed t-test. For each connection, we considered
284 the first 3 clusters as they represent the strongest effect. In summary, we applied FDR on $16 \times$
285 $3 = 48$ tests.

286

287 *(B) Dissociating directional information from sustained activity*

288 We converted the r values from correlation analysis to z-values using the Fisher-z-
289 transformation formula. The critical value that corresponds to $p=0.05$ for Fisher-z-transformed
290 Pearson correlation coefficient with $n=20$ is Fisher-z=0.48. We used cluster-based statistics
291 (Maris and Oostenveld, 2007), 1,000 permutations, and two-tailed one-sample t-tests against the
292 critical Fisher-z value of 0.48. To generate the null distribution, we shuffled the subjects and
293 calculated the r values and converted them to Fisher-z-values at each permutation. To correct for
294 8 connections, we applied FDR correction at the $q_{\text{FDR}} = 0.05$ threshold. For each connection, we
295 considered the first positive cluster, which means the decoding accuracies of top-down and
296 bottom-up effects are positively correlated.

297

298 **Results**

299

300 *Information flow from temporal areas to IFG*

301 We tested for across-areal generalization by training the classifier on MTG and STG
302 evoked response activity and then testing this classifier on IFG activity. Any cluster above the
303 diagonal shows how earlier time in temporal areas affect future time in frontal, which we interpret
304 as reflecting bottom-up-type influences. We observed this pattern in five out of 6 significant
305 connections (**Figure 3**). These patterns included from influences from the left pSTG to left pIFG,
306 left pMTG to left pIFG, left aMTG to left aIFG, right pSTG to right pIFG, and right pMTG to right
307 pIFG. The left pSTG influenced pIFG processing at multiple time intervals starting from 250ms
308 and extended later to 500ms (**Figure 3A**). From the left pMTG to pIFG and from the left aMTG to
309 aIFG, there was a continuous bottom-up effect from 50ms to 450 and 500ms respectively (**Figure**
310 **3C-D**). In the case of connectivity patterns from the right pSTG to pIFG and from the right pMTG
311 to pIFG, the bottom-up effects were more discontinuous (**Figure 3E-F**).

312

313 *Information flow from IFG to temporal areas*

314 Analogously to the above section, we tested for across-areal generalization by training the
315 classifier on IFG evoked response activity and then testing this classifier on STG and MTG
316 activity. We found significantly larger than chance level (50%) accuracy in 6 connections corrected
317 for multiple comparisons (**Figure 4**). These included the left aIFG to left aSTG, left aIFG to left
318 aMTG, left pIFG to left pMTG, right pIFG to right pMTG, right pIFG to right pSTG, and right aIFG
319 to right aSTG. The temporal generalization dynamics were different in each connection. When
320 the cluster expands above the diagonal, it shows that at each time, the classifier trained in IFG is
321 predictive of future time points in temporal-cortex areas. We interpret these kinds of patterns as
322 reflecting top-down influences from IFG to temporal areas. From left aIFG to left aSTG and aMTG,

323 there were effects up to 250ms and 450ms respectively that started as early as 50ms and were
324 sustained for at least 200ms (**Figure 4A-B**). The effect from left pIFG to pMTG started later around
325 250ms and continued for about 200ms and affected time interval after 450ms (**Figure 4C**). The
326 earliest frontal effect seemed to start from right pIFG to pMTG and pSTG (**Figure 4D-E**), where
327 the influence on pMTG lasted longer time up to 400ms, whereas in pSTG up to around 150ms.
328 There was also a continuous effect from right aIFG to aSTG around 200ms for a short duration.
329 Furthermore, from right aIFG to aSTG, there was a small effect before 200ms.

330 Those connections that are significant in both directions are plotted side-by-side in **Figure**
331 **5** for comparing the temporal specificity of the top-down and bottom-up effects.

332

333 *Dissociating directional information from sustained activity*

334 Out of eight tested connections, the connection between the left pSTG and pIFG was
335 significant, with $p=0.04$. In **Figure 6**, the Fisher-Z-transformed values of the correlations of top-
336 down and bottom-up decoding accuracies across all subjects for this connection and the
337 significant cluster within are shown.

338

339 **Discussion**

340 In this study, we used a novel approach to investigate bottom-up and top-down influences
341 between inferior frontal and temporal cortex areas, using source estimates of event-related MEG
342 responses to low-predictability vs. high-predictability nouns.

343 Our rationale rests on the utility of temporal generalization methods in multivariate
344 classification of brain data from specific brain areas: The idea is that when the classifier
345 performance exceeds chance level in the testing area at future time points, this means that brain
346 activity in the training area contain information that helps predicting the LP vs HP condition future

347 time points in the testing area. By examining instances when the classifier training was based at
348 an earlier time period than the testing, we made inferences on potential directional influences in
349 language processing underlying N400 generation.

350 We present evidence for both bottom-up influences from STG/MTG to IFG and top-down
351 influences from IFG to STG/MTG in both hemispheres. The strongest bottom-up effects were
352 observed from the left pSTG/pMTG to the left pIFG and from the left aMTG to the left aIFG. In
353 parallel, the strongest top-down effects were from the left aIFG to the left aSTG/aMTG and from
354 the right pIFG to the right pSTG/pMTG. These results suggest that bottom-up and top-down
355 influences are transferred through both ventral and dorsal pathways, and that they are not
356 restricted to a certain path. The dorsal and ventral pathways are the two main structural pathways
357 supporting language processing. The ventral pathway connects the temporal cortex to inferior
358 frontal regions via the extreme fiber capsule system (EFCS) and the uncinate fascicle (UF) and
359 the dorsal pathway connects the posterior frontal area to posterior part of the temporal cortex via
360 the arcuate fascicle (AF) and the superior longitudinal fascicle (SLF) (Friederici, 2012). Moreover,
361 our results suggest that bottom-up influences are mostly left lateralized whereas top-down
362 influences are present in both hemispheres. In our previous study (Maess et al, 2016), focused
363 on the evoked responses of the verbs and the nouns, we observed a reduction of the N400
364 response for highly predicted nouns as expected and the opposite pattern for the noun-preceding
365 verbs. Highly predictive verbs yielded stronger N400 amplitude compared to less predictive verbs.
366 Enhanced activity for highly predictive relative to less predictive verbs has been interpreted to
367 reflect pre-activations of semantic features associated with the expected nouns. Therefore, it is
368 interesting that top-down influences start at very early latencies, almost immediately after the
369 stimulus onset. In contrast, the majority of bottom-up influences started at least with a 100 ms
370 delay. The finding is also in agreement with an interpretation that feedback from IFG to temporal
371 cortex is stronger for the LP condition than the HP condition, since integrating LP nouns in context

372 requires a stronger/longer availability of the noun than in the HP condition (Baggio and Hagoort,
373 2011; Hagoort, 2017; Mamashli et al., 2019b).

374 It is worth to note that top-down and bottom-up effects have distinct temporal patterns in
375 each connection, as evidenced by our analysis which dissociated directional information from
376 sustained activity. In the case of sustained activity and no temporal separation of top-down and
377 bottom-up effects, there should have been strong correlations between them. We found only in
378 one connection (left pSTG and left pIFG) for which such a correlation effect was present (Figure
379 6).

380 Thus, we conclude that in the five connections in which a significant effect was found in both
381 directions (Figure 5), bottom-up and top-down effects occurred at different time latencies.
382 Interestingly, the left pSTG-pIFG connection did not show a significant bidirectional effect, but
383 only a bottom-up one (Figure 3).

384 A number of competing models have been proposed on top-down and bottom-up
385 influences between temporal and frontal areas during sentence comprehension (Friederici 2012).
386 Verifying such models has been difficult due to the complications in estimating causality in human
387 recordings. Indeed, to date, only a few previous studies have estimated the causal connections
388 between temporal and frontal areas in predictive speech processing using more classic
389 techniques. Cope et al. (2017) found bi-directional fronto-temporal causal connections using
390 Granger causality in distinct frequency bands when spoken words were matched with visual
391 presentation. Using similar method in a reading task, Schoffelen et al. (2017) found a bottom-up
392 connection from pMTG to IFG and top-down and bottom-up connections between IFG and aMTG.
393 A recent study (Schroen et al., 2023) using a subset of our stimulus material investigated temporo-
394 frontal causal influences with a combined transcranial magnetic stimulation and
395 electroencephalography approach. Interestingly, using this completely different approach, they
396 also observed early bottom-up influences from left pSTG to left IFG and late top-down influences
397 (300-500ms) from left IFG to left pSTG. Consistent with these previous results, the present results

398 highlight the importance of bidirectional interactions between functionally specialized brain
399 regions to facilitate complex language processing (Friederici 2012). Our novel inter-regional
400 temporal generalization could facilitate quantitative testing of theoretical models proposed for
401 language processing in general (Hickok and Poeppel, 2004, 2007; Friederici, 2011) and N400
402 processing in particular (Lau et al., 2008).

403 Estimating top-down and bottom-up influences using neuroimaging data has been
404 challenging. One of the inherent properties of these connections is that bottom-up influences,
405 which originate at lower levels of the processing hierarchy, are stimulus-driven and time-locked.
406 In turn, top-down influences, which originate at higher hierarchical levels and associated with
407 cognitive processing, can be presumed to jitter in time and vary more prominently subject by
408 subject, for example, due to individual differences in cognitive capacities. The more pronounced
409 variability within and between individuals weakens the estimated representations of top-down
410 influences in time relative to bottom-up influences, making their quantitative estimation harder.
411 This could be one of the factors why in the present study, the average decoding accuracy was
412 stronger in analyses, which were trained at the lower and tested at the higher hierarchical levels
413 (i.e., predominantly bottom-up) than vice versa (i.e., predominantly top-down).

414 Consistent with the best practices of MEG/EEG research (Gross et al., 2013), the present
415 MEG data were preprocessed using a long-duration, steep-slope FIR filter designed with
416 frequency-domain techniques. This non-causal (delay-compensated) filter offers zero-phase and
417 zero-delay, making it well-suited for investigating event-related responses such as the N400. The
418 potential limitation of these non-causal filters is that they may introduce time leakage in both
419 forward and backward directions, which could slightly influence the onset and offset of effects.
420 However, in the present study, the temporal clusters of statistically significant effects spanned
421 several hundred milliseconds, which reduces the concern that the effect were significantly
422 influenced by the leakage problem. On the other hand, using alternative approaches such as
423 causal filters, which can avoid leakage from future (but not past) time points, may introduce delays

424 and phase distortion, making them suboptimal for studies of event-related effects in MEG or EEG.
425 Future research is therefore needed to evaluate how different filtering strategies affect the
426 decoding accuracy of inter-regional temporal generalization.

427

428 **Conclusion**

429 In summary, we implemented a novel method to estimate top-down (or feedback) and bottom-up
430 (or feedforward) influences using cross-regional temporal generalization in MEG decoding.
431 Aiming to understand the information flow in N400 generation in a simple language paradigm, we
432 found IFG feeding back to STG/MTG bilaterally and STG/MTG feeding forward to IFG left-
433 lateralized. Our results are consistent with the long-standing but empirically challenging notion
434 that dynamic top-down and bottom-up influences between IFG and temporal areas drive N400
435 generation.

436

437 **Data and Code Availability:** Data and code will be available upon request.

438

439 **Author Contributions:** F.M. conceived the study, designed the study, conducted the
440 experiments, analyzed the data, and wrote the manuscript. S.K., J.A., conceived the study,
441 designed the study, analyzed the data, and wrote the manuscript. A.F., B.M., and J.O. designed
442 the study, conducted the experiments, and wrote the manuscript, E.H., M.J., I.U, K.L, analyzed
443 the data and wrote the manuscript.

444

445

446 **References**

447

448 Badre D, Wagner AD (2007) Left ventrolateral prefrontal cortex and the cognitive control of
449 memory. *Neuropsychologia* 45:2883-2901.

450 Badre D, Poldrack RA, Pare-Blagoev EJ, Insler RZ, Wagner AD (2005) Dissociable controlled
451 retrieval and generalized selection mechanisms in ventrolateral prefrontal cortex. *Neuron*
452 47:907-918.

453 Baggio G, Hagoort P (2011) The balance between memory and unification in semantics: A
454 dynamic account of the N400. *Language and Cognitive Processes* 26:1338-1367.

455 Cichy RM, Pantazis D (2017) Multivariate pattern analysis of MEG and EEG: A comparison of
456 representational structure in time and space. *NeuroImage* 158:441-454.

457 Cope TE, Sohoglu E, Sedley W, Patterson K, Jones PS, Wiggins J, Dawson C, Grube M,
458 Carlyon RP, Griffiths TD, Davis MH, Rowe JB (2017) Evidence for causal top-down
459 frontal contributions to predictive processes in speech perception. *Nat Commun* 8:2154.

460 Dikker S, Pylkkanen L (2012) Predicting language: MEG evidence for lexical preactivation. *Brain*
461 *Lang.*

462 Engel AK, Fries P, Singer W (2001) Dynamic predictions: oscillations and synchrony in top-
463 down processing. *Nat Rev Neurosci* 2:704-716.

464 Federmeier KD (2007) Thinking ahead: the role and roots of prediction in language
465 comprehension. *Psychophys* 44:491-505.

466 Federmeier KD, Wlotko EW, De Ochoa-Dewald E, Kutas M (2007) Multiple effects of sentential
467 constraint on word processing. *Brain Res* 1146:75-84.

468 Fischl B, Sereno MI, Dale AM (1999a) Cortical surface-based analysis. II: Inflation, flattening,
469 and a surface-based coordinate system. *Neuroimage* 9:195-207.

470 Fischl B, Sereno MI, Tootell RB, Dale AM (1999b) High-resolution intersubject averaging and a
471 coordinate system for the cortical surface. *Hum Brain Mapp* 8:272-284.

472 Friederici AD (2011) The Brain Basis of Language Processing: From Structure to Function.
473 *Physiological reviews* 91:1357-1392.

474 Friederici AD (2012) The cortical language circuit: from auditory perception to sentence
475 comprehension. *Trends in Cognitive Sciences* 16:262-268.

476 Gramfort A, Luessi M, Larson E, Engemann DA, Strohmeier D, Brodbeck C, Parkkonen L,
477 Hämäläinen MS (2014) MNE software for processing MEG and EEG data. *Neuroimage*
478 86:446-460.

479 Granger CWJ, Hatanaka M (1964) *Spectral Analysis of Economic Time Series*. Princeton, NJ:
480 Princeton University Press.

481 Gross J, Baillet S, Barnes GR, Henson RN, Hillebrand A, Jensen O, Jerbi K, Litvak V, Maess B,
482 Oostenveld R, Parkkonen L, Taylor JR, van Wassenhove V, Wibral M, Schoffelen J-M

483 (2013) Good practice for conducting and reporting MEG research. *NeuroImage* 65:349-
484 363.

485 Hagoort P (2017) The core and beyond in the language-ready brain. *Neuroscience &*
486 *Biobehavioral Reviews* 81:194-204.

487 Halgren E, Dhond RP, Christensen N, Van Petten C, Marinkovic K, Lewine JD, Dale AM (2002)
488 N400-like magnetoencephalography responses modulated by semantic context, word
489 frequency, and lexical class in sentences. *Neuroimage* 17:1101-1116.

490 Hämäläinen MS, Sarvas J (1987) Feasibility of the homogeneous head model in the
491 interpretation of neuromagnetic fields. *Phys Med Biol* 32:91-97.

492 Hatamimajoumerd E, Talebpour A, Mohsenzadeh Y (2020) Enhancing multivariate pattern
493 analysis for magnetoencephalography through relevant sensor selection. *International*
494 *Journal of Imaging Systems and Technology* 30:473-494.

495 Hatamimajoumerd E, Ratan Murty NA, Pitts M, Cohen MA (2022) Decoding perceptual
496 awareness across the brain with a no-report fMRI masking paradigm. *Curr Biol* 32:4139-
497 4149 e4134.

498 Hickok G, Poeppel D (2004) Dorsal and ventral streams: a framework for understanding aspects
499 of the functional anatomy of language. *Cognition* 92:67-99.

500 Hickok G, Poeppel D (2007) The cortical organization of speech processing. *Nat Rev Neurosci*
501 8:393-402.

502 King JR, Dehaene S (2014) Characterizing the dynamics of mental representations: the
503 temporal generalization method. *Trends Cogn Sci* 18:203-210.

504 Kutas M, Hillyard SA (1980) Reading Senseless Sentences - Brain Potentials Reflect Semantic
505 Incongruity. *Science* 207:203-205.

506 Kutas M, Hillyard SA (1984) Brain Potentials during Reading Reflect Word Expectancy and
507 Semantic Association. *Nature* 307:161-163.

508 Kutas M, Hillyard SA (1989) An electrophysiological probe of incidental semantic association. *J*
509 *Cogn Neurosci* 1:38-49.

510 Kutas M, Federmeier KD (2011) Thirty years and counting: finding meaning in the N400
511 component of the event-related brain potential (ERP). *Annu Rev Psychol* 62:621-647.

512 Lau EF, Phillips C, Poeppel D (2008) A cortical network for semantics: (de)constructing the
513 N400. *Nature reviews Neuroscience* 9:920-933.

514 Lau EF, Holcomb PJ, Kuperberg GR (2013a) Dissociating N400 effects of prediction from
515 association in single-word contexts. *J Cogn Neurosci* 25:484-502.

516 Lau EF, Almeida D, Hines PC, Poeppel D (2009) A lexical basis for N400 context effects:
517 evidence from MEG. *Brain and language* 111:161-172.

518 Lau EF, Gramfort A, Hämäläinen MS, Kuperberg GR (2013b) Automatic semantic facilitation in
519 anterior temporal cortex revealed through multimodal neuroimaging. *J Neurosci*
520 33:17174-17181.

- 521 Lin FH, Belliveau JW, Dale AM, Hämäläinen MS (2006) Distributed current estimates using
522 cortical orientation constraints. *Hum Brain Mapp* 27:1-13.
- 523 Maess B, Herrmann CS, Hahne A, Nakamura A, Friederici AD (2006) Localizing the distributed
524 language network responsible for the N400 measured by MEG during auditory sentence
525 processing. *Brain Res* 1096:163-172.
- 526 Maess B, Mamashli F, Obleser J, Helle L, Friederici AD (2016) Prediction Signatures in the
527 Brain: Semantic Pre-Activation during Language Comprehension. *Front Hum Neurosci*
528 10:591.
- 529 Mamashli F, Hämäläinen M, Ahveninen J, Kenet T, Khan S (2019a) Permutation Statistics for
530 Connectivity Analysis between Regions of Interest in EEG and MEG Data. *Sci Rep*
531 9:7942.
- 532 Mamashli F, Khan S, Obleser J, Friederici AD, Maess B (2019b) Oscillatory dynamics of cortical
533 functional connections in semantic prediction. *Hum Brain Mapp* 40:1856-1866.
- 534 Mamashli F, Huang S, Khan S, Hämäläinen M, Ahveninen J (2019c) Modulation of phase
535 synchronization across fronto-parietal and temporal cortices during auditory attention. In:
536 *Cognitive Neuroscience Society, 25th Annual Meeting, March 23-26. San Fransisco, CA.*
- 537 Mamashli F, Huang S, Khan S, Hamalainen MS, Ahlfors SP, Ahveninen J (2020) Distinct
538 Regional Oscillatory Connectivity Patterns During Auditory Target and Novelty
539 Processing. *Brain Topogr* 33:477-488.
- 540 Mamashli F, Khan S, Hamalainen M, Jas M, Raij T, Stufflebeam SM, Nummenmaa A,
541 Ahveninen J (2021a) Synchronization patterns reveal neuronal coding of working
542 memory content. *Cell Rep* 36:109566.
- 543 Mamashli F, Khan S, Bharadwaj H, Michmizos K, Ganesan S, Garel KA, Ali Hashmi J, Herbert
544 MR, Hamalainen M, Kenet T (2017) Auditory processing in noise is associated with
545 complex patterns of disrupted functional connectivity in autism spectrum disorder.
546 *Autism Res* 10:631-647.
- 547 Mamashli F, Kozhemiako N, Khan S, Nunes AS, McGuiggan NM, Losh A, Joseph RM,
548 Ahveninen J, Doesburg SM, Hamalainen MS, Kenet T (2021b) Children with autism
549 spectrum disorder show altered functional connectivity and abnormal maturation
550 trajectories in response to inverted faces. *Autism Res* 14:1101-1114.
- 551 Marinkovic K, Dhond RP, Dale AM, Glessner M, Carr V, Halgren E (2003) Spatiotemporal
552 dynamics of modality-specific and supramodal word processing. *Neuron* 38:487-497.
- 553 Maris E, Oostenveld R (2007) Nonparametric statistical testing of EEG- and MEG-data. *J*
554 *Neurosci Methods* 164:177-190.
- 555 Mohsenzadeh Y, Qin S, Cichy RM, Pantazis D (2018) Ultra-Rapid serial visual presentation
556 reveals dynamics of feedforward and feedback processes in the ventral visual pathway.
557 *Elife* 7.
- 558 Noppeney U, Price CJ, Penny WD, Friston KJ (2006) Two distinct neural mechanisms for
559 category-selective responses. *Cereb Cortex* 16:437-445.
- 560 Oldfield RC (1971) The Assessment and Analysis of Handedness: The Edinburgh Inventory.
561 *Neuropsychologia* 9:97-113.

562 Price CJ (2010) The anatomy of language: a review of 100 fMRI studies published in 2009. Ann
563 Ny Acad Sci 1191:62-88.

564 Pulvermüller F, Shtyrov Y, Ilmoniemi R (2005) Brain signatures of meaning access in action
565 word recognition. J Cogn Neurosci 17:884-892.

566 Pylkkanen L, McElree B (2007) An MEG study of silent meaning. J Cogn Neurosci 19:1905-
567 1921.

568 Salmelin R (2007) Clinical neurophysiology of language: the MEG approach. Clin Neurophysiol
569 118:237-254.

570 Schoffelen JM, Hulten A, Lam N, Marquand AF, Udden J, Hagoort P (2017) Frequency-specific
571 directed interactions in the human brain network for language. Proc Natl Acad Sci U S A
572 114:8083-8088.

573 Schroen JAM, Gunter TC, Numssen O, Kroczeck LOH, Hartwigsen G, Friederici AD (2023)
574 Causal evidence for a coordinated temporal interplay within the language network. Proc
575 Natl Acad Sci U S A 120:e2306279120.

576 Taulu S, Simola J (2006) Spatiotemporal signal space separation method for rejecting nearby
577 interference in MEG measurements. Phys Med Biol 51:1759-1768.

578 Taulu S, Kajola M, Simola J (2004) Suppression of interference and artifacts by the Signal
579 Space Separation Method. Brain topography 16:269-275.

580 Taylor WL (1953) "Cloze Procedure": A New Tool For Measuring Readability. Journalism Quart
581 30:415-433.

582 Van Essen DC, Dierker DL (2007) Surface-based and probabilistic atlases of primate cerebral
583 cortex. Neuron 56:209-225.

584 Wlotko EW, Federmeier KD (2012) So that's what you meant! Event-related potentials reveal
585 multiple aspects of context use during construction of message-level meaning.
586 NeuroImage 62:356-366.

587

588

589 **Figure captions**

590

591 **Figure 1:** ROIs and sub-regions or sub-ROIs in left and right hemisphere.

592

593 **Figure 2:** A schematic display of the method. (A) Examples of ROIs and sub-ROIs in pIFG and
594 pSTG. SVM classifier is trained on four features from four sub-ROIs activity in pIFG to classify LP
595 from HP conditions and then tested on the four features extracted from pSTG sub-ROI activity.
596 Similarly, the same process was done from pSTG to pIFG. (B) SVM classifier is trained at each
597 time point of pIFG activity and tested on all time points of pSTG. The accuracy of model from
598 pSTG test data is used to create temporal generalization matrix. Here, one time point t_0 and t_1 are
599 shown as an example.

600

601 **Figure 3:** Temporal generalization decoding matrix averaged over all subjects. The white contour
602 indicates significant decoding values against the chance level. SVM classifier is (A) trained on the
603 left pSTG and tested on the left pIFG, (B) trained on the left pMTG and tested on the left pIFG,
604 (C) trained on the right aSTG and tested on the right aIFG, and (D) trained on the right pMTG and
605 tested on the right pIFG, (E) trained on the right pSTG and tested on the right pIFG, (F) trained
606 on the right pMT and tested on the right pIFG. (G) The ROIs and the significant connections from
607 (A) to (F) are displayed in a cortical surface representation.

608

609 **Figure 4:** Temporal generalization decoding matrix averaged over all subjects. The white contour
610 indicates significant decoding values against the chance level. The SVM classifier is (A) trained
611 on the left aIFG and tested on the left aSTG, (B) trained on the left aIFG and tested on the left
612 aMTG, (C) trained on the left pIFG and tested on the left pMTG, (D) trained on the right pIFG and

613 tested on the right pMTG, (E) trained on the right pIFG and tested on the right pSTG, and (F)
614 trained on the right aIFG and tested on right aSTG. (G) The ROIs and the significant connections
615 from (A) to (F) are displayed in a cortical surface representation.

616

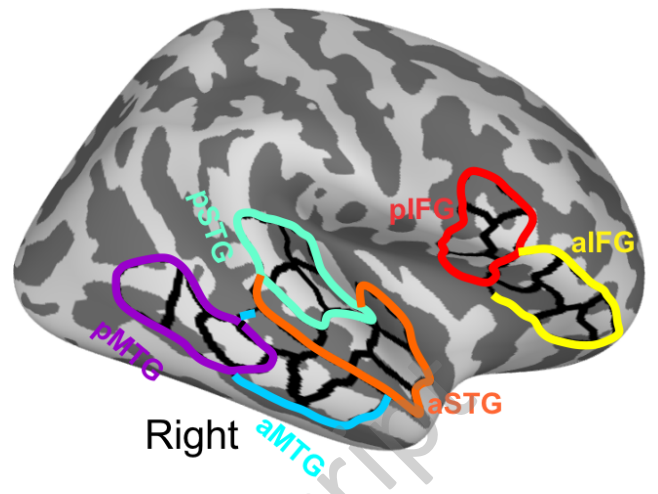
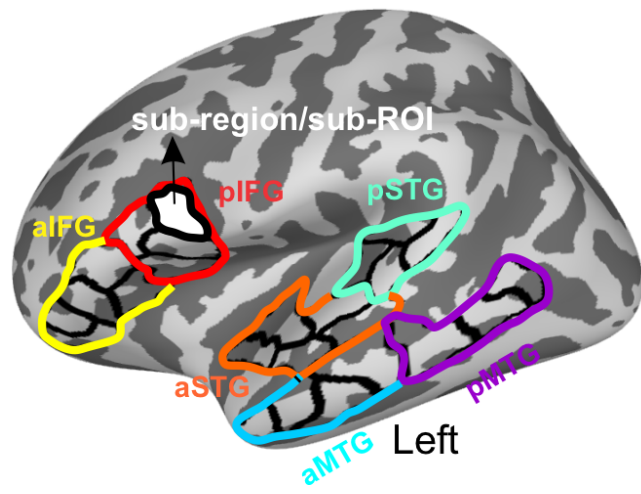
617 **Figure 5:** Significant connections that are bi-directional. The left panel shows the bottom-up
618 effects, and the right panel is the top-down effects.

619

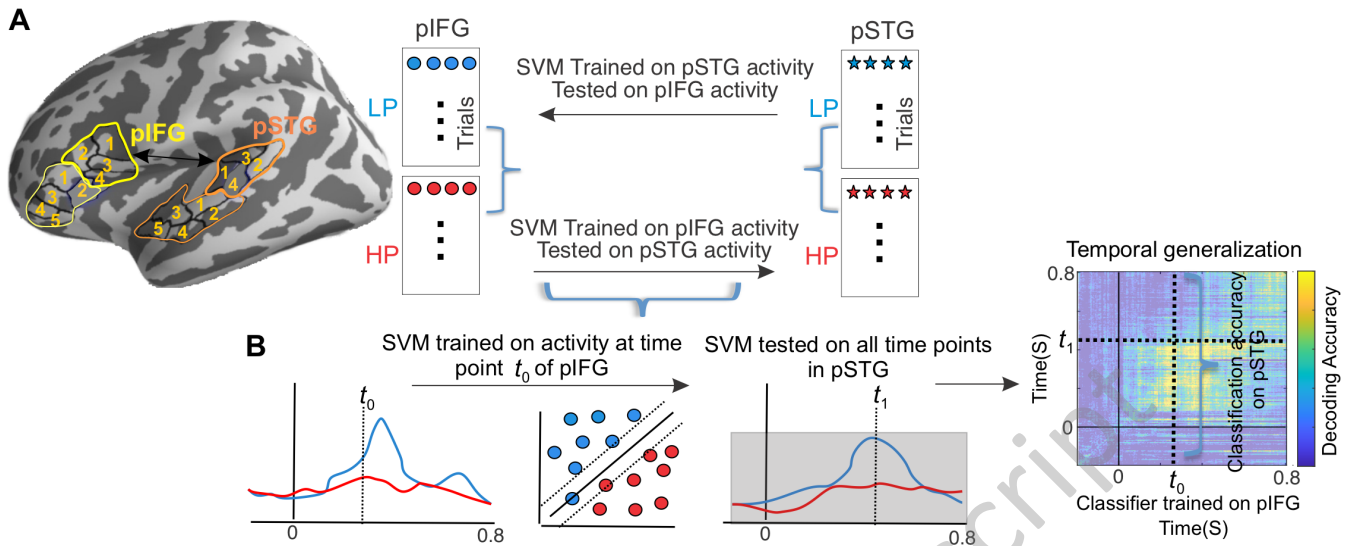
620 **Figure 6:** Fisher-z-transformed correlation values of decoding values of top-down and bottom-up
621 effects for the connection between left-pSTG and pIFG.

622

JNeurosci Accepted Manuscript

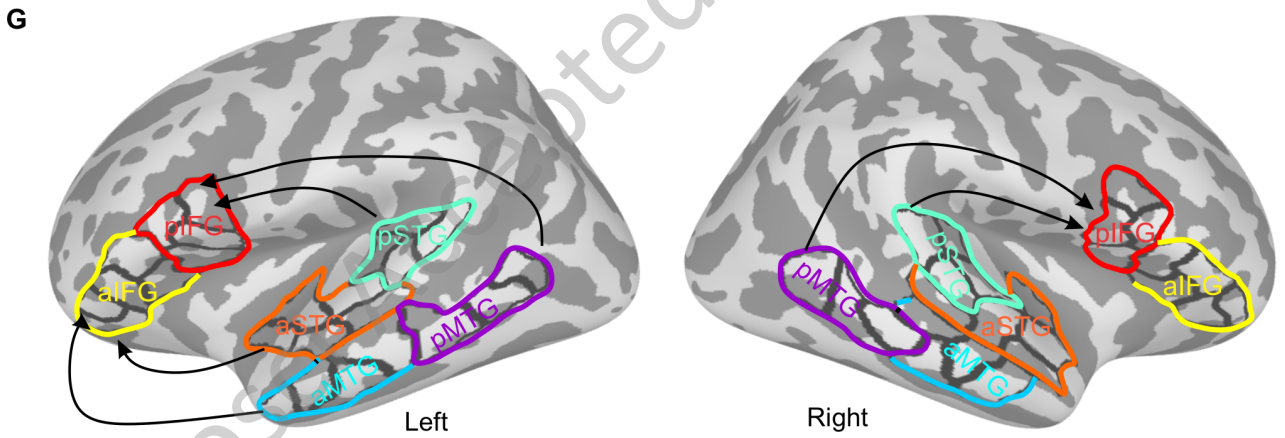
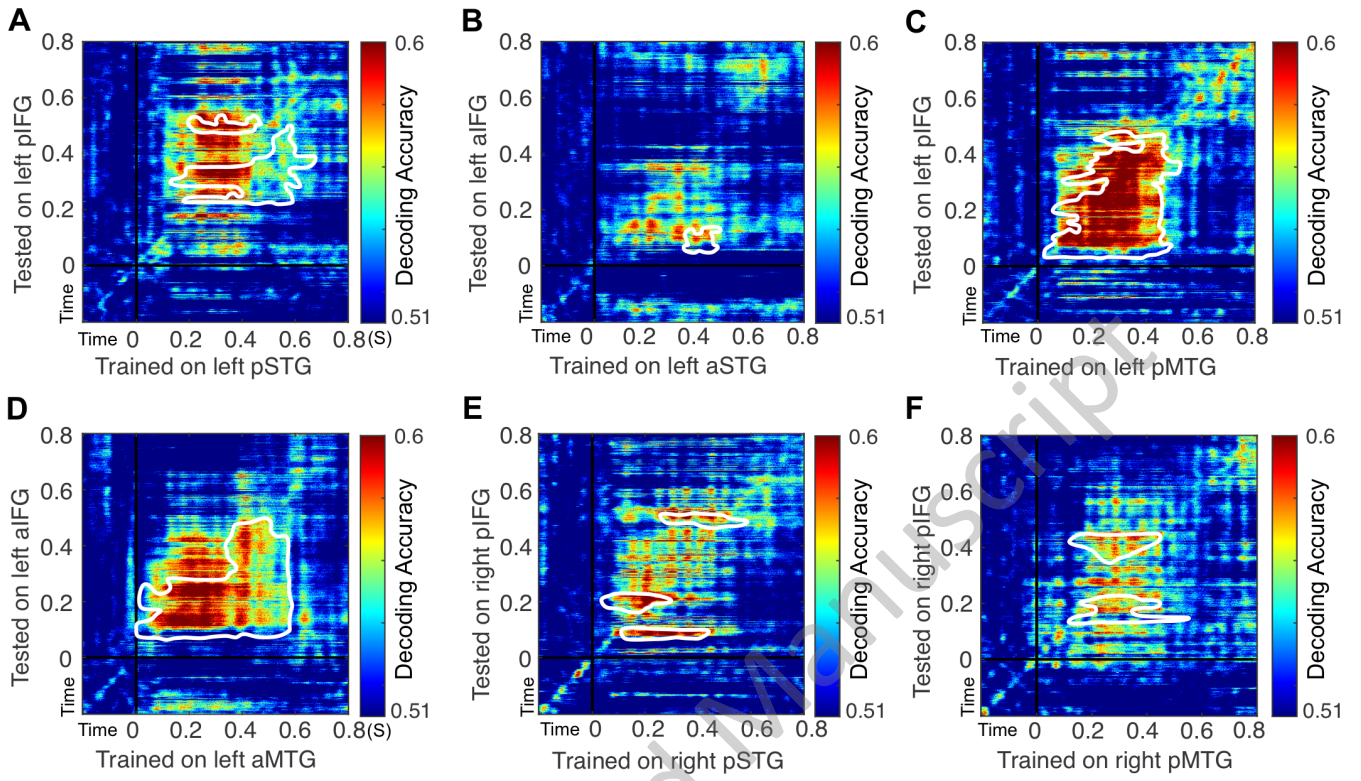


JNeurosci Accepted Manuscript

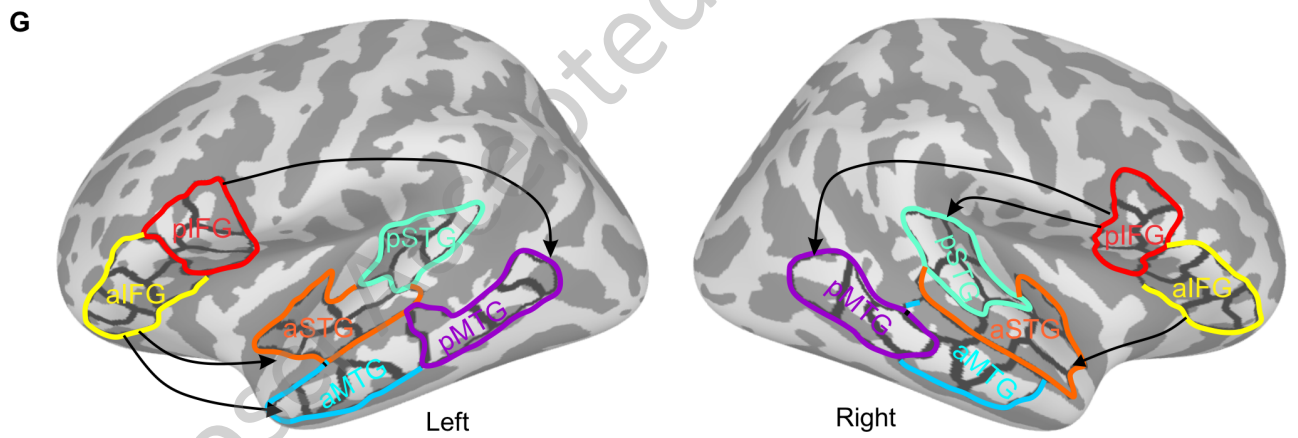
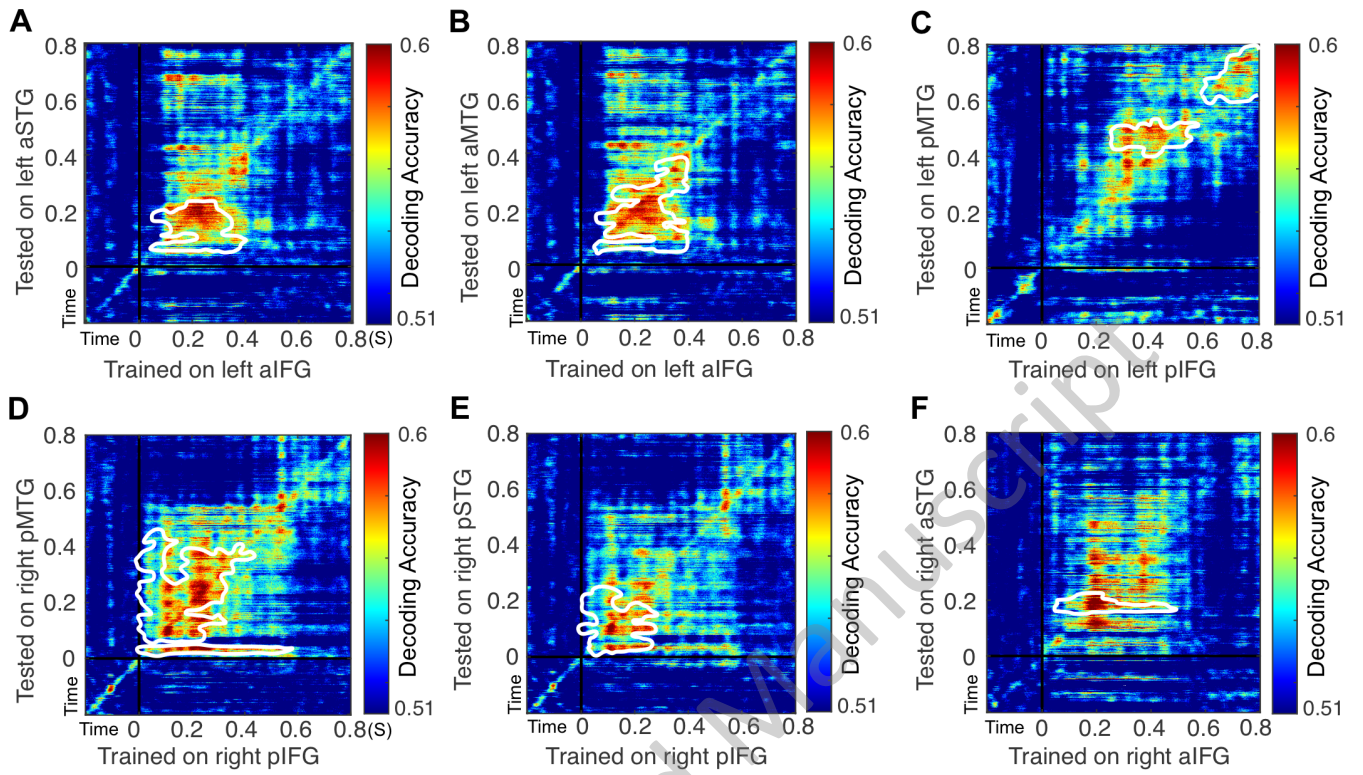


JNeurosci Accepted Manuscript

Classifier Trained on Temporal and Tested on Inferior Frontal

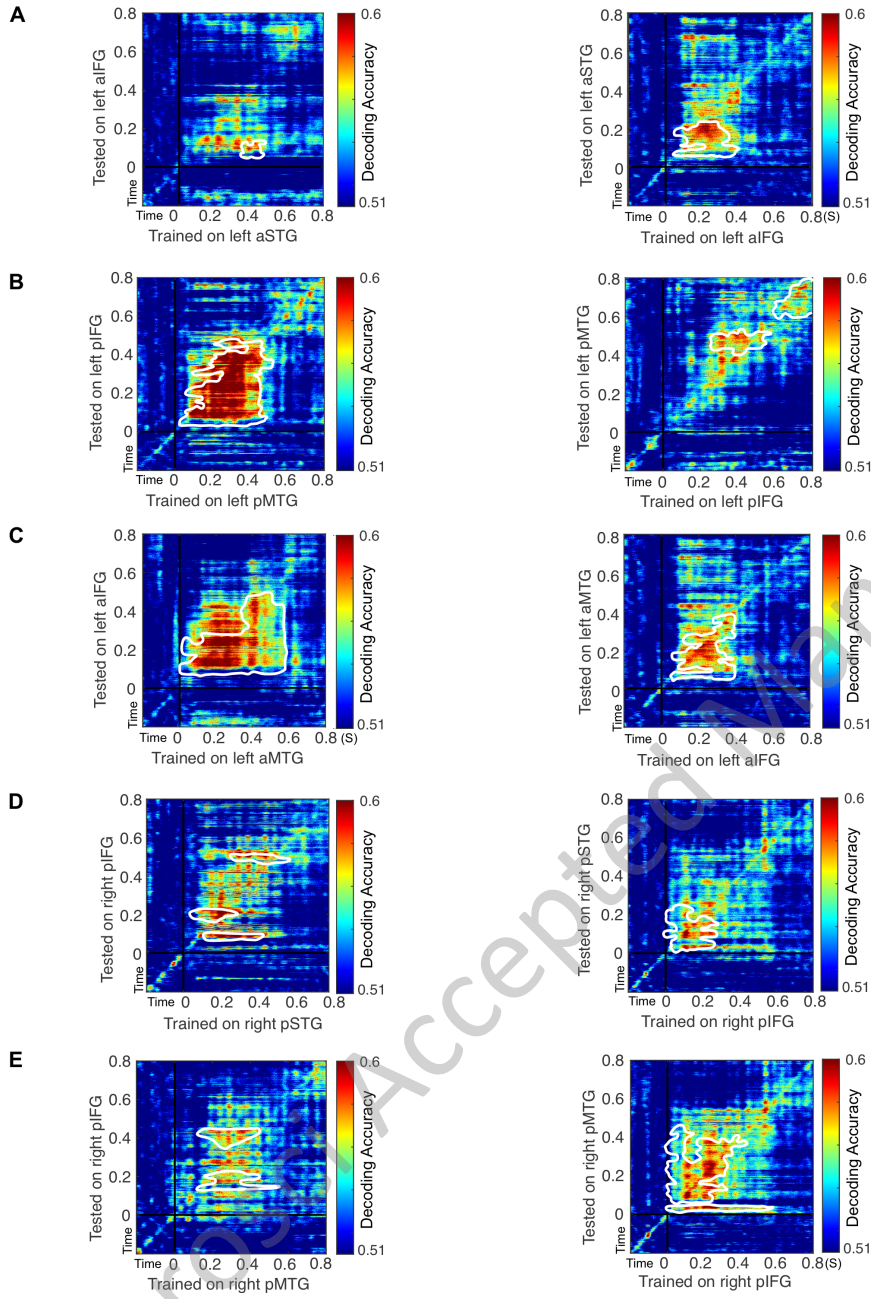


Classifier Trained on Inferior Frontal and Tested on Temporal

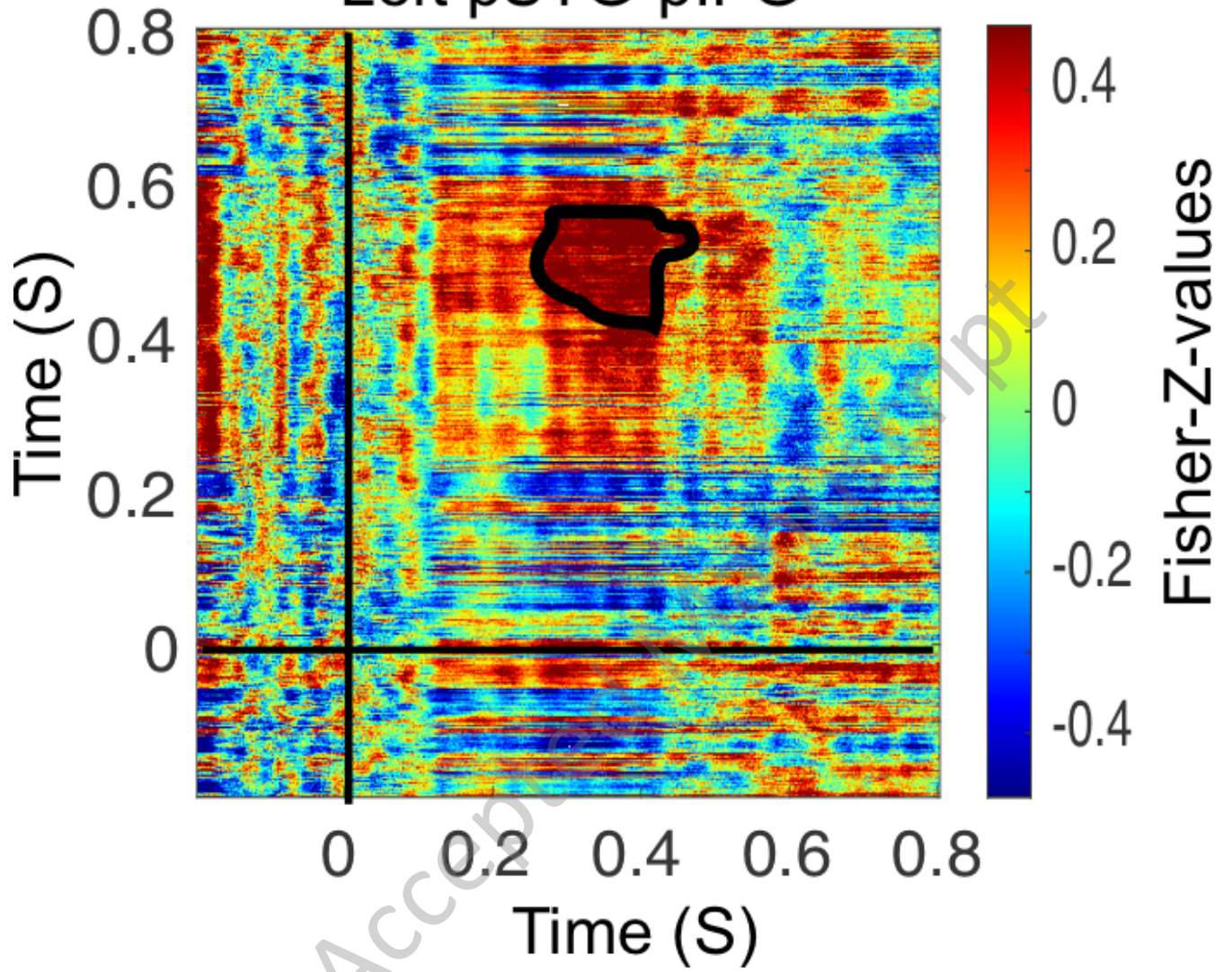


Trained on Temporal and Tested on Inferior Frontal

Trained on Inferior Frontal and Tested on Temporal



Left pSTG-pIFG



JNeurosci Accepted Article